Neurobiology of Disease

Sodium-Dependent Vitamin C Transporter 2 Deficiency Causes Hypomyelination and Extracellular Matrix Defects in the Peripheral Nervous System

Burkhard Gess,[1] Dominik Röhr,[1,2] Robert Fledrich,[3] Michael W. Sereda,[3,4] Ilka Kleffner,[1] Anne Humberg,[1] Johanna Nowitzki,[1] Jan-Kolja Strecker,[1] Hartmut Halfter,[1] and Peter Young[1]

Departments of [1]Neurology and [2]Biology, University of Münster, 48149 Münster, Germany, [3]Department of Neurogenetics, Max-Planck Institute for Experimental Medicine, 37075 Göttingen, Germany, and [4]Department of Clinical Neurophysiology, University of Göttingen, 37075 Göttingen, Germany

Ascorbic acid (vitamin C) is necessary for myelination of Schwann cell/neuron cocultures and has shown beneficial effects in the treatment of a Charcot-Marie-Tooth neuropathy 1A (CMT1A) mouse model. Although clinical studies revealed that ascorbic acid treatment had no impact on CMT1A, it is assumed to have an important function in peripheral nerve myelination and possibly in remyelination. However, the transport pathway of ascorbic acid into peripheral nerves and the mechanism of ascorbic acid function in peripheral nerves *in vivo* remained unclear.

In this study, we used sodium-dependent vitamin C transporter 2-heterozygous (SVCT2 $^{+/-}$) mice to elucidate the functions of SVCT2 and ascorbic acid in the murine peripheral nervous system. SVCT2 and ascorbic acid levels were reduced in SVCT2 $^{+/-}$ peripheral nerves. Morphometry of sciatic nerve fibers revealed a decrease in myelin thickness and an increase in G-ratios in SVCT2 $^{+/-}$ mice. Nerve conduction velocities and sensorimotor performance in functional tests were reduced in SVCT2 $^{+/-}$ mice. To investigate the mechanism of ascorbic acid function, we studied the expression of collagens in the extracellular matrix of peripheral nerves. Here, we show that expression of various collagen types was reduced in sciatic nerves of SVCT2 $^{+/-}$ mice. We found that collagen gene transcription was reduced in SVCT2 $^{+/-}$ mice but hydroxyproline levels were not, indicating that collagen formation was regulated on the transcriptional and not the posttranslational level. These results help to clarify the transport pathway and mechanism of action of ascorbic acid in the peripheral nervous system and may lead to novel therapeutic approaches to peripheral neuropathies by manipulation of SVCT2 function.

Introduction

Ascorbic acid is thought to have a major function in peripheral nerve myelination based on the consistent and reproducible observation that ascorbic acid is necessary for *in vitro* myelination in Schwann cell/dorsal root ganglion (DRG) cocultures (Olsen and Bunge, 1986; Eldridge et al., 1987). Ascorbic acid was shown to induce the formation of a collagen- and laminin-containing extracellular matrix *in vitro*, that—in turn—was necessary for myelination in Schwann cell/DRG cocultures (Carey and Todd, 1987; Eldridge et al., 1989). Particularly, collagen V was shown to be important for myelination as inhibition of collagen V or its receptor, glypican-1, significantly reduced myelination *in vitro* (Chernousov et al., 2006). However, the function of ascorbic acid for peripheral nerve myelination has not been shown *in vivo*, and the effects of ascorbic acid on peripheral nerve extracellular matrix *in vivo* remain elusive.

Because of its promyelinating function *in vitro*, ascorbic acid was used in an experimental treatment study on PMP22-transgenic mice as an animal model for Charcot-Marie-Tooth neuropathy 1A (CMT1A) (Passage et al., 2004). This animal study showed a functional and histopathological improvement in PMP22-transgenic mice treated with ascorbic acid. Because of these positive results, various clinical trials of ascorbic acid administration in CMT1A were started. None of these trials showed a significant benefit of ascorbic acid in the treatment of CMT1A patients (Burns et al., 2009; Micallef et al., 2009; Verhamme et al., 2009). Recently, the largest and first study to be conducted over 2 years reported no significant differences between ascorbic acid and placebo groups (Pareyson et al., 2011). However, despite successful elevation of ascorbic acid levels in blood of ascorbic acid-treated patients (Burns et al., 2009; Micallef et al., 2009), there is no data on ascorbic acid uptake in peripheral nerves. The transport mechanism of ascorbic acid into the peripheral nervous system has not been determined so far. In our previous work we demonstrated the expression and transport activity of sodium-dependent vitamin C transporter 2 (SVCT2) in Schwann cell cultures (Gess et al., 2010). SVCT2 is thought to be the main

Received July 7, 2011; revised Aug. 30, 2011; accepted Sept. 29, 2011.

Author contributions: B.G., I.K., and P.Y. designed research; B.G., D.R., R.F., A.H., J.N., J.-K.S., and H.H. performed research; B.G., R.F., M.W.S., H.H., and P.Y. analyzed data; B.G. wrote the paper.

The authors declare no conflicts of interest.

We are grateful for funding from Deutsche Forschungsgemeinschaft (DFG Grant GE 2249/1-1) and Innovative Medizinische Forschung (IMF Grant LO 110704). M.W.S. was supported by the Bundesministerium für Bildung und Forschung (Grant FKZ01ES0801) and the AFM (Grant 15037). We thank Dr. Nussbaum, University of California, San Francisco for the kind provision of SVCT2 $^{+/-}$ mice. We thank Dr. Sorokin, University of Muenster, and Dr. Wagener, University of Cologne, for the kind gift of antibodies. We thank Dr. Schilling for professional advice on electrophysiological methods.

Correspondence should be addressed to Prof. Peter Young, Klinik und Poliklinik für Neurologie, Universitätsklinikum Münster, Albert-Schweitzer Strasse 33, 48149 Münster, Germany. E-mail: young@uni-muenster.de.

DOI:10.1523/JNEUROSCI.3457-11.2011

 0270-6474/11/3117180-13$15.00/0

ascorbic acid transport protein in the brain and was shown to be expressed in cultured neurons, neuroblastoma cells, hypothalamic glia cells, and choroid epithelia cells (Angelow et al., 2003; Garcia Mde et al., 2005; Caprile et al., 2009). The SVCT2-*null* mouse dies of brain hemorrhages and lung failure shortly after birth (Sotiriou et al., 2002). The ascorbic acid content in brains of newborn SVCT2-*null* pups was shown to be close to zero.

In this study we show reduced ascorbic acid concentrations in peripheral nerves of SVCT2 $^{+/-}$ mice leading to decreased myelin thickness, locomotor impairment, and defects within the extracellular matrix of peripheral nerves. Deleterious effects of SVCT2 inhibition on collagen synthesis and myelination were confirmed in Schwann cell cultures and Schwann cell/DRG cocultures. These results help to clarify the transport mechanism of ascorbic acid into the peripheral nervous system and the mechanism of ascorbic acid action in myelination *in vivo*, potentially leading to novel treatment approaches to CMT1A and other demyelinating neuropathies through direct manipulation of SVCT2.

Materials and Methods

Mouse breeding

All animal studies and procedures have been approved by the local governmental authorities (State Office for Nature, Environment, and Consumer Protection, North Rhine-Westphalia, Germany; AZ 8.87-50.10.36.08.297) and were conducted in accordance with the European Convention for Animal Care and Ethical Use of Laboratory Animals. The number of animals was kept to a minimum needed.

Animals were maintained in standard laboratory conditions with a 12 h/12 h light-dark cycle and were allowed free access to food and water. SVCT2 $^{+/-}$ mice were kindly provided by Dr. Nussbaum (University of California, San Francisco, CA). Since SVCT $^{-/-}$ mice are not viable (Sotiriou et al., 2002), SVCT $^{+/-}$ mice were bred by mating SVCT2 $^{+/+}$ with SVCT2 $^{+/-}$ mice leading to ~50% SVCT2 $^{+/-}$ offspring. Mice were genotyped by tail cuts and PCR. Primer sequences for PCR were as follows: wild-type forward, 5′-TAATCCTGGCTATCCTCGTG-3′; wild-type reverse, 5′-CATCTGTGCGTGCATAGTAGC-3′; knock-out forward, 5′-GATTGCACGCAGGTTCTCC-3′; knock-out reverse, 5′-GCCAACGCTATGTCCTGATA-3′. Mice of either sex were used for experiments.

Behavioral studies and electrophysiology

All behavioral tests and electrophysiological measurements were performed by a trained investigator blinded toward the genotypes of the mice.

Rotarod. Motor performance was measured on a rotating bar using the Rotarod device (TSE Systems). Animals were trained for 2 d to get used to the rotating bar and tested on three consecutive days. Each day, five runs were conducted with each animal. Mice were placed on the Rotarod, which accelerated starting from 5 to 52 rounds per min over 400 s. The time each mouse stayed on the rotating rod was measured and recorded.

Gait analysis. Gait analysis was conducted using a walking track 1 m in length and 10 cm in width laid out with paper strips. Mice were trained one or two times before the first measurement. The hindpaws of mice were dipped in nontoxic paint (Pelikan). From the foot prints, the stride lengths of at least six strides were measured. Only regular walking intervals (no stopping or curving) were scored. The stride variability was calculated by subtracting the shortest stride from the longest stride, as described previously (Fleming and Chesselet, 2005). The angles between foot steps and walking direction were measured with the image analysis software Analysis.

Hot plate test. Mice were placed on temperature-controlled plate heated to 50°C and the time was measured to the nearest 0.1 s until a lick of a hindpaw or a jump of the mouse. If the mouse showed no response after 60 s, the test was stopped. The mouse was immediately taken off the plate and placed back in its home cage.

Electrophysiology. Electrophysiology was performed on mice at postnatal day (P)100. Mice were anesthetized with ketamine hydrochloride/xylazine hydrochloride (100 mg/kg body weight/ 8 mg/kg body weight). The body temperature of the mice was adjusted to 37°C using a controlling circuit with a rectal temperature probe and a heating pad on which the mice were laid. Local temperature near the sciatic nerve was controlled to be at 37°C using a needle thermometer, which was inserted near the nerve at the thigh. A pair of steel needle electrodes (Schuler Medizintechnik) was placed subcutaneously along the nerve at the sciatic notch (proximal stimulation). A second pair of electrodes was placed along the tibial nerve above the ankle (distal stimulation). Supramaximal square wave pulses lasting 100 ms were delivered using a Toennies NeuroScreen system (Jaeger). Compound muscle action potential (CMAP) was recorded from the intrinsic foot muscles using steel electrodes. Both amplitudes and latencies of CMAP were determined. The distance between the two sites of stimulation was measured alongside the skin surface with fully extended legs and nerve conduction velocities (NCVs) were calculated automatically from sciatic nerve latency measurements.

Histology

For histology, SVCT2 $^{+/-}$ and SVCT2 $^{+/+}$ animals, 60 and 300 d after birth (P60 and P300), were used. In deep ketamine/xylazine anesthesia the animals were intracardially perfused with isotonic saline followed by a fixative solution (4% PFA, 2% glutaraldehyde in 0.1 M cacodylate buffer, pH 7.4). Sciatic nerves were dissected, postfixed for 24 h at 4°C, osmicated for 2 h in 2% osmium tetroxide at room temperature, washed in distilled H_2O several times, dehydrated in ascending acetone, and finally embedded in Spurr's medium (Young et al., 2002). Semi-thin sections (0.5 μm) were cut using an Ultracut 200 microtome (Leica), stained with alkaline toluidine blue, and subsequently analyzed by measuring axon diameter and fiber diameter on three sections per sciatic nerve. An average of 300 fibers were measured per optical field on three sections per sciatic nerve, amounting to 900 fibers measured per animal and 2700 fibers per genotype and age group. For electron microscopy, ultrathin sections were cut (70 nm), mounted on copper grids, and contrasted with uranyl citrate and lead citrate. Grids were viewed and photographed on a Philips transmission electron microscope (Philips).

Cell culture

Rat Schwann cell cultures were prepared according to a previously reported method (Vroemen and Weidner, 2003) with modifications as described previously (Gess et al., 2008). Schwann cells were passaged 3–4 times before being used for experiments. Dorsal root ganglion neurons from embryonal rats at gestational age E16 and Schwann cell/DRG cocultures were prepared and cultured as described previously (Eldridge et al., 1987; Gess et al., 2008). For *in vitro* myelination, Schwann cells were added to 3-week-old DRG neurons depleted of endogenous Schwann cells and fibroblasts. The day after addition of Schwann cells, ascorbic acid (50 μg/ml) was added to the medium. After 2 weeks, cocultures were fixed and analyzed by immunohistochemistry to myelin basic protein (MBP). For phloretin inhibition, 100 μM phloretin (Sigma-Aldrich) was added to the culture medium. For siRNA experiments, rat Schwann cells were transfected with siRNA oligonucleotides as described previously (Gess et al., 2008). Briefly, $5*10^5$ Schwann cells/well were plated on 6 well culture plates. On the following day, Schwann cells were transfected. Schwann cells were incubated with 1 ml of serum-free OptiMEM (Invitrogen). Transfection reactions with 16 μl of siRNA solution (20 μM stock) and 8 μl of Oligofectamine (Invitrogen) in 256 μl of OptiMEM were prepared. Two hundred eighty microliters of transfection reaction mixture were added dropwise to the 1 ml of OptiMEM on Schwann cells. After incubation at 37°C and 7% CO_2 overnight, transfection reactions were replaced by Schwann cell medium. Two days after transfection, Schwann cells were harvested for Western blot or quantitative real-time PCR (qRT-PCR) analysis. siRNA oligonucleotides were as follows: CAUCCUGUCUUUAGAUAAdTdT for SVCT2 and UUCUCCGAA CGUGUCACGUdTdT as a nonsense control (Qiagen).

Immunohistochemistry

For immunohistochemistry, mice were anesthetized with ketamine/xylazine and killed by cervical dislocation. Sciatic nerves were dissected and embedded in Tissue-Tek OCT (Sakura Finetek). Ten micrometer sections were cut with a cryotome (Leica CM 3050). Slides were fixed with 4% paraformaldehyde for 1 h at room temperature. Schwann cell/DRG

cocultures were fixed with 4% paraformaldehyde at 4°C for 15 min. Slides were rinsed and incubated with blocking solution containing 10% goat serum, 1% BSA, and 0.1% Triton X-100 (Sigma-Aldrich) in PBS for1 h. Slides were incubated with primary antibodies at 4°C overnight and with secondary antibodies at room temperature for1 h. Primary antibodies used in this study were as follows: SVCT2 (1:100, Santa Cruz Biotechnology), SMI32 (1:500, Covance); S100 (1:1000, DakoCytomation); MBP (1:200, DakoCytomation); collagen IV and collagen V (both 1:100, Millipore); collagen XXVIII (1:1000, kindly provided by Dr. Wagener, University of Cologne, Cologne, Germany), laminin 2 (1:1000, kindly provided by Dr. Sorokin, University of Münster); E-cadherin (1: 200, BD Biosciences); fibronectin (1:500, Abcam). Secondary antibodies were as follows: goat anti-rabbit A488, goat anti-mouse A488, goat anti-mouse A594, and goat anti-rabbit A594 (all 1:200, Invitrogen). Slides were mounted with Vecta-Shield mounting medium containing nuclear counterstain DAPI (Vector Laboratories) and covered with coverslips. Slides were viewed with a Leica fluorescence microscope (Leica) and photographed with a SPOT cooled digital camera.

Western blot

Sciatic nerves were lysed with lysis buffer containing 25 mM Tris, 1 mM $NaVO_3$, 1% SDS, and 2 mM EDTA. Lysates were homogenized using an ultrasonicator (Dr. Hielscher GmbH), followed by several passes through a syringe with a 21 gauge needle. Lysates were centrifuged (4°C, 10,000 × *g*) for 15 min. Cell culture media were precipitated by 20% trichloroacetic acid (Sigma-Aldrich) on ice for 15 min, followed by centrifugation (4°C with 10,000 × *g*) for 15 min. Protein concentrations were determined by the Bradford method. Samples of 10 μg of protein were loaded onto 10% SDS-polyacrylamide gels. After electrophoresis, proteins were transferred to PVDF membranes (Millipore) in a wet blot chamber (Bio-Rad) at 4°C overnight. Membranes were stained with Ponceau Red (Bio-Rad), destained with Tris-buffered saline containing 0.05% Tween 20 (Sigma-Aldrich) (TBST), blocked with 4% milk powder, and incubated with the primary antibodies SVCT2, SVCT1 (both 1:1000,Santa Cruz Biotechnology), collagen IV, collagen V (both 1:1000, Millipore), collagen XVIII (1:20,000, Dr. Wagener), or β-actin (1: 15,000,Santa Cruz Biotechnology) at 4°C overnight. Membranes were washed with TBST and incubated with HRP-conjugated secondary antibodies (1:20,000, Invitrogen) at room temperature for1 h. Bound antibodies were visualized using chemiluminescence (Pierce) and x-ray films. Densitometric analysis was done with ImageJ image processing software (NIH). Collagen band intensities were normalized by respective β-actin bands, and intensity of SVCT2 $^{+/-}$ bands was computed in percentage of wild-type bands, which were set to 100%.

Quantitative real-time reverse transcription PCR

RNA purification was carried out with the RNeasy Mini Kit (Qiagen) according to the manufacturer's instructions. Briefly, cells were lysed with buffer containing 1% β-mercaptoethanol (v/v) and homogenized by passing through an RNase-free syringe with a 21 gauge needle and subsequent ultrasonication. After reverse transcription with the QuantiTect Reverse Transcription kit (Qiagen), qRT-PCR was performed with real-time primer assays for P0 [Myelin Protein Zero (MPZ)], PMP22, collagens IV (alpha 1), V (alpha 1), XV (alpha 1), and XXVIII (alpha 1), and GAPDH (all Qiagen). Real-time PCR reactions were run with SYBR Green (Fermentas) according to the manufacturer's protocol. Gene expression was related to expression of GAPDH as a housekeeping gene. GAPDH as a housekeeping gene showed only minor variability in cycle threshold values of <1% in our assays and was used previously as a housekeeping gene in a landmark paper on the PMP22-overexpressing rat (Sereda et al., 1996). Relative expression analysis of target genes was done using the relative expression software tool REST-MCS version 2, which uses the efficiency-corrected comparative crossing point method to estimate a sample expression ratio (Pfaffl, 2001; Pfaffl et al., 2002).

Biochemical assays

For determination of ascorbic acid concentration and malondialdehyde (MDA) assays, sciatic nerves were dissected, immediately frozen in liquid nitrogen, and stored at −80°C until further use. Nerves were lysed in distilled H_2O on ice for 15 min and triturated with a plastic mortar (Eppendorf). Lysates were mixed with an equal volume of 6% $HClO_4$ and 2% HPO_3 (Sigma-Aldrich) and incubated on ice for 15 min followed by centrifugation for 15 min (4°C, 10,000 × *g*). Ascorbic acid concentration in supernatants was detected by reverse-phase, high-pressure liquid chromatography with UV detection at 243 nm.

Hydroxyproline assays were done as described previously (Woessner, 1961). Briefly, nerve lysates were hydrolyzed with 6 N HCl at 130°C for 3 h. Hydrolysates were resuspended in distilled water (dH_2O) and mixed with 1.4% chloramine T solution (1.41 g of chloramine T (Merck), 20 ml of dH_2O, 30 ml of methyl cellosolve (Sigma-Aldrich), and 50 ml of buffer (50 g of citric acid monohydrate, 120 g of sodium acetate trihydrate, 34 g of sodium hydroxide, and 12 ml of glacial acetic acid in a final volume of 1 L dH_2O), incubated for 20 min at room temperature, stopped with 3.15 M perchloric acid, mixed with Ehrlich's reagent (Sigma-Aldrich), and incubated for 20 min at 60°C. After cooling in tap water, absorbance was read at 557 nm. The concentration of hydroxyproline was calculated from a standard curve from standards freshly prepared with *trans*-4-hydroxy-L-proline (Sigma-Aldrich).

Malondialdehyde assays were performed based on a previously described protocol (Harrison et al., 2010a). Briefly, nerve lysates were mixed 1:1 with 0.02 M thiobarbituric acid and incubated for 35 min at 95°C followed by 10 min at 4°C. Malondialdehyde was measured by spectrophotometry at 532 nm. Malondialdehyde standards were prepared by hydrolysis of tetramethoxypropane (Sigma-Aldrich) with 0.1 M HCl at 99°C for 5 min as described previously (Karatas et al., 2002).

Statistical analysis

In experiments with two groups and one variable, Student's *t* test was used to test for significant differences between means. In experiments with more than two groups and one variable, one-way ANOVA and Tukey's *post hoc* test was used. In experiments with two or more groups and two variables, two-way ANOVA and Bonferroni's *post hoc* test was used. Results are shown as means of at least three independent experiments ± SD. Group sizes (n) and significance levels (p) are given in the figure legends. p values are denoted as follows: $^{*}p < 0.05$, $^{**}p < 0.01$, $^{***}p < 0.001$. Results were considered to be statistically significant if $p < 0.05$.

Results

SVCT2 $^{+/-}$ mice show reduced SVCT2 expression and ascorbic acid concentration in peripheral nerves

SVCT2 $^{-/-}$ mice are not viable due to brain hemorrhages and lung failure. SVCT2 $^{+/-}$ mice, however, are viable and show reduced vitamin C concentrations in several tissues in adulthood (Sotiriou et al., 2002). To investigate whether SVCT2 $^{+/-}$ mice show reduced expression of SVCT2 in peripheral nerves, sciatic nerves of SVCT2 $^{+/-}$ were analyzed by qRT-PCR, immunohistochemistry, and Western blotting. qRT-PCR of sciatic nerves of mice at postnatal days 60 and 300 (P60 and P300), showed significant reductions of SVCT2 mRNA in SVCT2 $^{+/-}$ compared to SVCT2 $^{+/+}$ mice (Fig. 1*A*). Correspondingly, SVCT2 protein levels were reduced in lysates of sciatic nerves at P60 and P300 as detected by Western blots (Fig. 1*B*). Western blots further showed that SVCT1 was not compensatorily upregulated, but rather weakly expressed in both SVCT $^{+/-}$ and wild-type sciatic nerves (Fig. 1*B*). On cryosections, reduced immunoreactivity with SVCT2 antibodies was shown in SVCT2 $^{+/-}$ sciatic nerves compared to wild types (Fig. 1*C*).

Next, ascorbic acid levels were measured to assess whether ascorbic acid concentrations in sciatic nerves were reduced as a consequence of reduced SVCT2 enzyme. As shown in Figure 1*D*, ascorbic acid concentrations were significantly reduced at P20, P60, and P300 in SVCT2 $^{+/-}$ sciatic nerves compared to controls. Ascorbic acid concentrations in wild-type peripheral nerves were slightly lower than those reported for brain tissue (Harrison et al., 2010c), which are known to be very high compared to other organs and blood (Harrison and May, 2009).

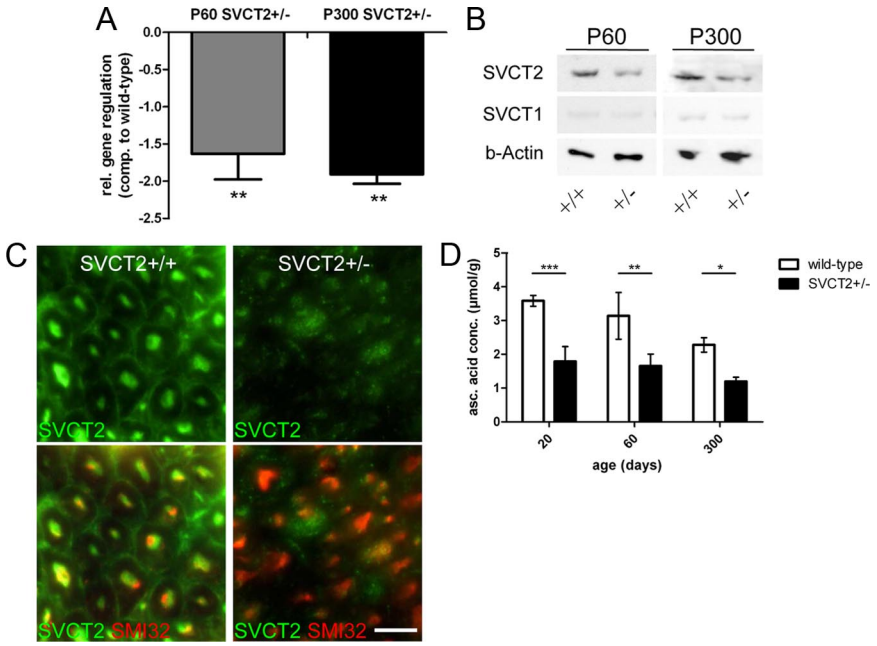

Figure 1. SVCT2 expression and vitamin C concentrations are reduced in SVCT2 $^{+/-}$ sciatic nerves. ***A***, Real-time reverse transcription PCR of mRNA extracts of sciatic nerves from SVCT2 $^{+/-}$ mice and wild-type controls at ages P60 and P300 was performed for SVCT2 and GAPDH for normalization. Results are shown as relative changes (rel.) of GAPDH-normalized SVCT2 expression ratios in SVCT2 $^{+/-}$ mice compared (comp.) to wild-type mice. qRT-PCR showed significant downregulation of SVCT2 at both P60 and P300 (P60 and P300: $^{**}p < 0.01$, $n = 3$). ***B***, Western blots of sciatic nerve lysates of SVCT2 $^{+/-}$ and wild-type control mice at ages P60 and P300 was performed and membranes were incubated with SVCT1 and SVCT2 antibodies. Actin was used as a marker of protein loading. Western blots showed reduced SVCT2 protein expression in SVCT2 $^{+/-}$ compared to wild-type sciatic nerves. SVCT1 was not changed, showing that SVCT1 is not compensatorily upregulated. ***C***, Cross-sections of sciatic nerves of wild-type (left) and SVCT2 $^{+/-}$ (right) mice were stained with SVCT2 (green) and neurofilament (SMI32, red) antibodies. Immunohistochemistry showed reduced expression of SVCT2 in SVCT2 $^{+/-}$ sciatic nerves (scale bar, 5 μm). ***D***, Ascorbic acid concentrations (asc. acid conc.) in peripheral nerve lysates from SVCT2 $^{+/-}$ and wild-type mice at ages P20, 60, and 300 were measured by high-pressure liquid chromatography. Ascorbic acid levels were markedly reduced in SVCT2 $^{+/-}$ compared to wild type at all time points (P20: $^{***}p < 0.001$, $n = 3$; P60: $^{**}p < 0.01$, $n = 3$; P300: $^{*}p < 0.05$, $n = 3$).

Together, these data show a reduction of SVCT2 mRNA and protein, leading to reduced ascorbic acid uptake into sciatic nerves of SVCT2 $^{+/-}$ mice.

Peripheral nerve myelin sheath thickness is decreased in SVCT2 $^{+/-}$ mice

Several studies *in vitro* showed ascorbic acid as a prerequisite for myelination of peripheral nerve axons (Olsen and Bunge, 1986; Eldridge et al., 1987, 1989). Since peripheral nerves in SVCT2 $^{+/-}$ mice showed reduced ascorbic acid levels *in vivo*, we were interested in finding whether this would cause demyelination. In toluidine blue-stained semi-thin sections (Fig. 2 *A*, *B*) and electron micrographs (Fig. 2*C*, *D*), a generally reduced myelin thickness in SVCT2 $^{+/-}$ nerves compared to controls was observed. No severely demyelinated axons or onion bulbs characteristic of active demyelination or demyelinating neuropathy-like CMT1A (Low et al., 1978) could be found. Toluidine blue-stained semi-thin sections were analyzed morphometrically. Axon diameter, fiber diameter, myelin thickness, and G-ratio (axon diameter/fiber diameter) were determined for each fiber of a cross section. Morphometry showed significantly reduced myelin thickness in SVCT2 $^{+/-}$ mice compared to wild-type controls at both P60 and P300 (Fig. 2*E*). Axon diameters, however, were unchanged (Fig. 2*F*). In SVCT2 $^{+/-}$ mice, G-ratios were significantly elevated compared to those of wild-type animals (Fig. 2*G*), indicating a hypomyelination of SVCT2 $^{+/-}$ peripheral nerves. The distribution of myelin thickness of fibers was skewed toward thinner myelin in SVCT2 $^{+/-}$ nerves (Fig. 2*H*), while the distribution of axon diameters was unchanged (Fig. 2*I*). The scatter plot of G-ratios versus axon diameters showed higher G-ratios in SVCT2 $^{+/-}$ mice compared to wild-types mice regardless of axon diameter, indicating that hypomyelination in SVCT2 $^{+/-}$ nerves was not restricted to a certain group of fibers (Fig. 2*J*). On high-resolution electron micrographs (Fig. 2 *K*, *L*), individual myelin wraps within the myelin sheath could be identified and counted. Significant reductions in the average number of myelin wraps per myelin sheath were shown in SVCT2 $^{+/-}$ compared to wild-type mice at both P60 and P300 (Fig. 2*M*). It should be noted that the number of myelin wraps in our analysis was relatively high compared to previous data by other groups (Cosgaya et al., 2002). This may be due to the relatively high age groups in our studies (P60 and P300) as opposed to P6 in Cosgaya et al. (2002). Myelin wrapping progresses until the adult age (Garratt et al., 2000).

The number of axons per mm ^{2} was not significantly different in SVCT2 $^{+/-}$ mice compared to wild-type mice (Fig. 2*N*). However, the percentage of myelinated fibers was reduced in SVCT2 $^{+/-}$ sciatic nerves (Fig. 2*O*). The number of Remak bundles (bundles of nonmyelinated fibers) was not significantly changed between SVCT2 $^{+/-}$ and wild-type mice, although a trend toward an increase in SVCT2 $^{+/-}$ mice was found (Fig. 2*P*). However, the number of axons per Remak bundle was significantly increased in SVCT2 $^{+/-}$ mice compared to wild-types (Fig. 2*Q*). The size distribution of Remak bundles was shifted toward Remak bundles with more axons in SVCT2 $^{+/-}$ mice compared to wild-type mice (data not shown).

To study the molecular architecture of nodes of Ranvier and the internodal lengths of peripheral nerve fibers, we analyzed single teased fibers of SVCT2 $^{+/-}$ and wild-type mice. Teased fibers showed no differences in the specific location of the nodal sodium channels (Fig. 2*R*, *S*), the paranodal potassium channel $K_V1.2$ (Fig. 2*T*, *U*), or the juxtaparanodal marker Caspr (Fig. 2*V*, *W*). Phase contrast images and internodal MBP staining (Fig. 2*X*, *Y*) showed no focal demyelinations or tomaculae. Lengths of internodes were measured on merged images of phase contrast and immunofluorescence to Na^+ channels. No difference in internodal lengths of SVCT2 $^{+/-}$ and wild-type fibers was observed (data not shown).

Overall, these results demonstrate a defect in peripheral nerve myelination of SVCT2 $^{+/-}$ mice causing a reduction in myelin thickness and a shift toward nonmyelinated axons in Remak bundles, but no significant changes in axon diameter or axon density.

SVCT2 $^{+/-}$ mice show deficits in sensorimotor function and nerve conduction studies

To assess functional effects of the hypomyelination observed in SVCT2 $^{+/-}$ mice, we tested motor function by Rotarod and gait analysis as well as sensory function by the hot plate test.

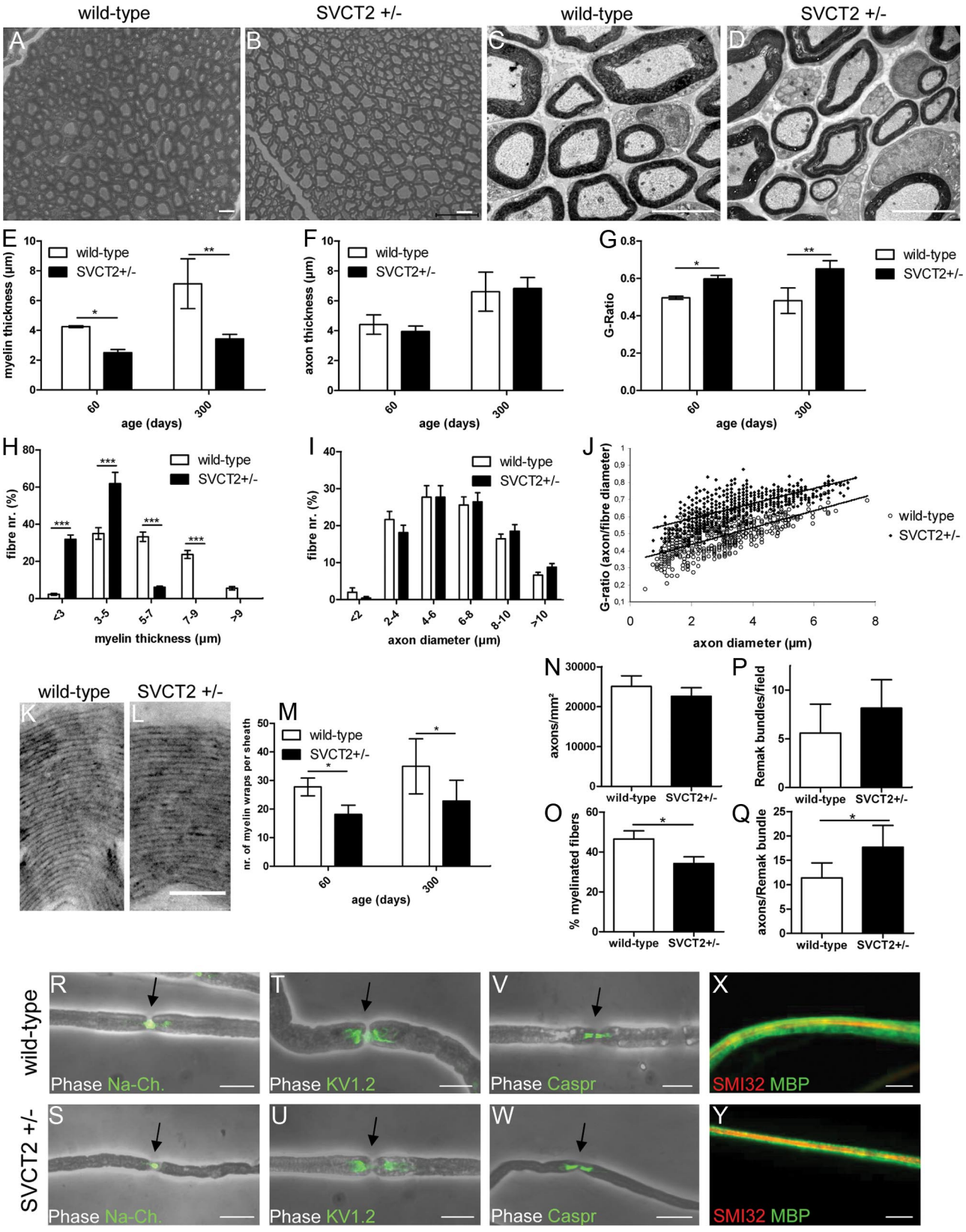

Figure 2. Peripheral nerves of SVCT2 $^{+/-}$ mice show thinner myelin and increased G-ratios but unaffected axon diameters. Sciatic nerves of SVCT2 $^{+/-}$ mice and wild-type controls were processed for histology by semi-thin toluidine blue-stained sections, ultrathin electron microscopy sections, and teased fiber analysis. ***A–D***, SVCT2 $^{+/-}$ nerves showed thinner myelin sheaths (***B***, ***D***) compared to wild type nerves (***A***, ***C***) in semi-thin toluidine-blue stained sections (***A***, ***B***) and electron micrographs (***C***, ***D***). ***E–G***, Semi-thin toluidine blue-stained sections at P60 and P300 were analyzed by morphometry. ***E***, Morphometry demonstrated significantly reduced myelin thickness in SVCT2 $^{+/-}$ compared to wild-type mice at both time points (P60: $*p < 0.05$, $n = 3$; P300: $**p < 0.01$, $n = 3$). ***F***, Axon diameters were unchanged in SVCT2 $^{+/-}$ nerves (P60: nonsignificant, $n = 3$; P300: nonsignificant, $n = 3$). ***G***, Corresponding to reduced myelin thickness, G-ratios (axon diameter/fiber diameter) were increased in SVCT2 $^{+/-}$ compared to wild-type mice (P60: $*p < 0.05$, $n = 3$; P300: $**p < 0.01$, $n = 3$). ***H–J***, Distributions of myelin thickness, axon diameters, and G-ratios of representative nerves from P300 mice are shown. ***H***, The distribution of myelin thickness was skewed to the left in SVCT2 $^{+/-}$ nerves ($*p < 0.001$, $n = 3$). (*Figure legend continues.*)

SVCT2 $^{+/-}$ mice showed a decrease in the time on the accelerating Rotarod compared to wild-type controls at P60 (Fig. 3*A*). At P300 there was a trend toward a reduced Rotarod performance of SVCT2 $^{+/-}$ mice that, however, was not statistically significant (Fig. 3A). At P300, both wild-type and SVCT2 $^{+/-}$ mice performed significantly worse than at P60. This age-dependent effect may have obscured differences between the genotypes in the elderly mice at P300. Gait analysis showed a significant reduction of stride length in SVCT2 $^{+/-}$ mice compared to controls both at P60 and P300 (Fig. 3*B*). Furthermore, stride length variability was increased in SVCT2 $^{+/-}$ mice compared to wild-type mice at both time points (Fig. 3*C*). Walking tracks were also analyzed for the angles between foot steps and walking direction. Representative walking tracks are shown in Figure 3, *D* and *E*. Step angles were wider in SVCT2 $^{+/-}$ compared to wild-type mice (Fig. 3*F*). To assess the sensory function of SVCT2 $^{+/-}$ mice, the well established hot plate test was used. The hot plate test showed a significant increase of the response time in SVCT2 $^{+/-}$ compared to wild-type control mice, indicating an impairment of nociception (Fig. 3*G*).

Nerve conduction studies of the sciatic nerves were performed to assess electrophysiological changes in SVCT2 $^{+/-}$ mice. Representative traces are shown in Figure 3, *H* and *I*. Nerve conduction studies showed a significant reduction of nerve conduction velocity in SVCT2 $^{+/-}$ mice compared to wild-type mice, while the amplitudes of compound muscle action potentials, CMAPs, were not significantly reduced (Fig. 3*J*). CMAP configuration was dispersed in SVCT2 $^{+/-}$ mice (Fig. 3*I*). Partial conduction block, defined as a $\geq$50% reduction of proximal compared to distal CMAP amplitudes, was found in two mice of the SVCT2 $^{+/-}$ group, and none of the wild-type group (Fig. 3*J*). Complete conduction blocks were not found.

Altogether, these data point toward a demyelinating/hypomyelinating neuropathy with reduced nerve conduction velocities causing sensorimotor deficits in SVCT2 $^{+/-}$ mice.

Extracellular matrix components are reduced in peripheral nerves of SVCT2 $^{+/-}$ mice

Ascorbic acid is known to play an important role in collagen synthesis (Booth and Uitto, 1981; Murad et al., 1981; Tajima and Pinnell, 1982). An ascorbic acid-induced, collagen-containing extracellular matrix is necessary for myelination in Schwann cell/DRG cocultures *in vitro* (Eldridge et al., 1987, 1989; Chernousov et al., 2006). *In vivo* evidence for this mechanism is lacking to this date. Since SVCT2 $^{+/-}$ mice show reduced ascorbic acid concentrations and hypomyelination in sciatic nerves, we were interested in studying the extracellular matrix in peripheral nerves of SVCT2 $^{+/-}$ mice.

First, longitudinal sections of sciatic nerves of SVCT2 $^{+/-}$ and wild-type control mice were stained by Gomori's stain. In these stainings, a slight disorganization of the collagen fibrils in SVCT2 $^{+/-}$ nerves could be observed (Fig. 4*A*). The epineurium of SVCT2 $^{+/-}$ nerves was colored more faintly by Gomori's stain (Fig. 4*A*, arrowheads) and its continuity was partially disrupted (Fig. 4*A*, asterisk).

Gomori's staining is a nonspecific technique to analyze collagen structures since it stains all types of collagen and allows no differentiation between specific collagen types. Hence, we sought to study collagens more sensitively and specifically by Western blots and immunohistochemistry. To analyze collagen and laminin expression on a whole-tissue level, Western blots of sciatic nerve lysates were prepared and stained with antibodies for specific collagen types or laminin-2. Marked reductions of collagen IV, V, and XXVIII, as well as slight reductions of laminin-2, could be observed in SVCT2 $^{+/-}$ mice compared to wild-type mice (Fig. 4*B*). Densitometric analysis of collagen bands showed significant downregulation of collagen IV, V, XXVIII, and laminin-2 (40, 41, 60, and 79% of control) in SVCT2 $^{+/-}$ sciatic nerves compared to wild-type sciatic nerves (Fig. 4*C*).

To specifically visualize different collagen types and laminin-2, sections of sciatic nerves were stained with antibodies against collagen XXVIII, V, and laminin-2. Collagen XXVIII immunoreactivity was diminished in SVCT2 $^{+/-}$ nerves compared to controls (Fig. 4*D–I*, *D′–I′*). Stainings with collagen V antibodies also revealed a reduction in collagen V immunoreactivity in SVCT2 $^{+/-}$ nerves compared to wild-type controls (Fig. 4*J–O*, *J′–O′*). Collagen XXVIII and V in the extracellular matrix, as shown by fibronectin costaining, were reduced in SVCT2 $^{+/-}$ compared to control nerves (Fig. 4*F*, *G*, *F′*, *G′*, *L*, *M*, *L′*, *M′*, insets). Also collagen XXVIII and V at nodes of Ranvier, as identified by costaining to E-cadherin, were markedly reduced (Fig. 4*H*, *I*, *H′*, *I′*, *N*, *O*, *N′*, *O′*, insets). Furthermore, a slight reduction of laminin 2 staining was observed in SVCT2 $^{+/-}$ nerves (Fig. 4*P–U*, *P′–U′*).

Together, these results illustrate deficiencies of extracellular matrix components in nerves of SVCT2 $^{+/-}$ mice.

Expression of Myelin Protein Zero and collagens is reduced in SVCT2 $^{+/-}$ nerves

To investigate the expression of myelin genes in SVCT2 $^{+/-}$ and wild-type control nerves, quantitative real-time PCR was performed. qRT-PCR signals were normalized by GAPDH. Results are shown as changes compared to wild-type control (Fig. 5).

qRT-PCR assays consistently showed a downregulation of MPZ mRNA in SVCT2 $^{+/-}$ mice compared to wild-type controls at both P60 and P300 (Fig. 5*A*). Interestingly, no significant changes in expression of PMP22 could be observed. At P60, an insignificant trend toward an increase in PMP22 mRNA was observed. At P300, PMP22 levels were largely unchanged in SVCT2 $^{+/-}$ sciatic nerves compared to wild-type controls.

Since we found deficiencies in various collagen types of SVCT2 $^{+/-}$ mice, especially type V, and knowing that collagen formation can be regulated by ascorbic acid not only through

←

(*Figure legend continued.*) ***I***, The distribution of axon diameters was not affected in SVCT2 $^{+/-}$ compared to controls. ***J***, The scatter plot of G-ratios over axon diameters showed a shift toward higher G-ratios in SVCT2 $^{+/-}$ nerves while the slope of the linear regression was unchanged. ***K***, ***L***, Individual myelin wraps within myelin sheaths could be observed and counted on high-magnification electron micrographs (36,000×) from wild-type (***K***) and SVCT2 $^{+/-}$ (***L***) sciatic nerves. ***M***, Quantification of myelin wraps demonstrated significant reductions in SVCT2 $^{+/-}$ mice compared to wild-type mice at both P60 and P300 (P60: $*p < 0.05$, $n = 3$; P300: $**p < 0.01$, $n = 3$). ***N***, The number of axons per mm ^{2} was not significantly different between SVCT2 $^{+/-}$ and wild-type nerves (P300: $p =$ nonsignificant, $n = 3$). ***O***, The percentage of myelinated fibers was reduced in SVCT2 $^{+/-}$ nerves (P300: $*p < 0.05$, $n = 3$). ***P***, The number of Remak bundles per visual field was not significantly different between SVCT2 $^{+/-}$ and wild-type nerves (P300: $p =$ nonsignificant, $n = 3$). ***Q***, The number of axons per Remak bundle was increased in SVCT2 $^{+/-}$ nerves (P300: $*p < 0.05$, $n = 3$). ***R–Y***, Single fiber analysis of teased fibers. Merged images of phase contrast and fluorescence-labeled markers (green) are shown in ***R–W***; merged images of myelin basic protein (green) and neurofilament (SMI32, red) are shown in ***X*** and ***Y***. Immunoreactivities to sodium channels (Na-Ch.) (***R***, ***S***), Kv1.2-channels (***T***, ***U***), and Caspr (***V***, ***W***) in nodes of Ranvier, paranodes, and juxtaparanodes, respectively, were unchanged between SVCT2 $^{+/-}$ and wild-types. MBP stainings of teased fibers confirmed the observation of thinner myelin sheaths (***X***, ***Y***). On MBP stainings or phase contrast images of teased fibers, no focal demyelinations or tomaculae could be observed. For morphometry, an average of 300 fibers per section were counted on three sections per nerve. For myelin wraps, an average of 100 fibers per nerve were analyzed. Three animals were analyzed per genotype and age group. Scale bars: ***A–D***, ***R–Y***, 10 μm; ***L***, ***M***: 1 μm.

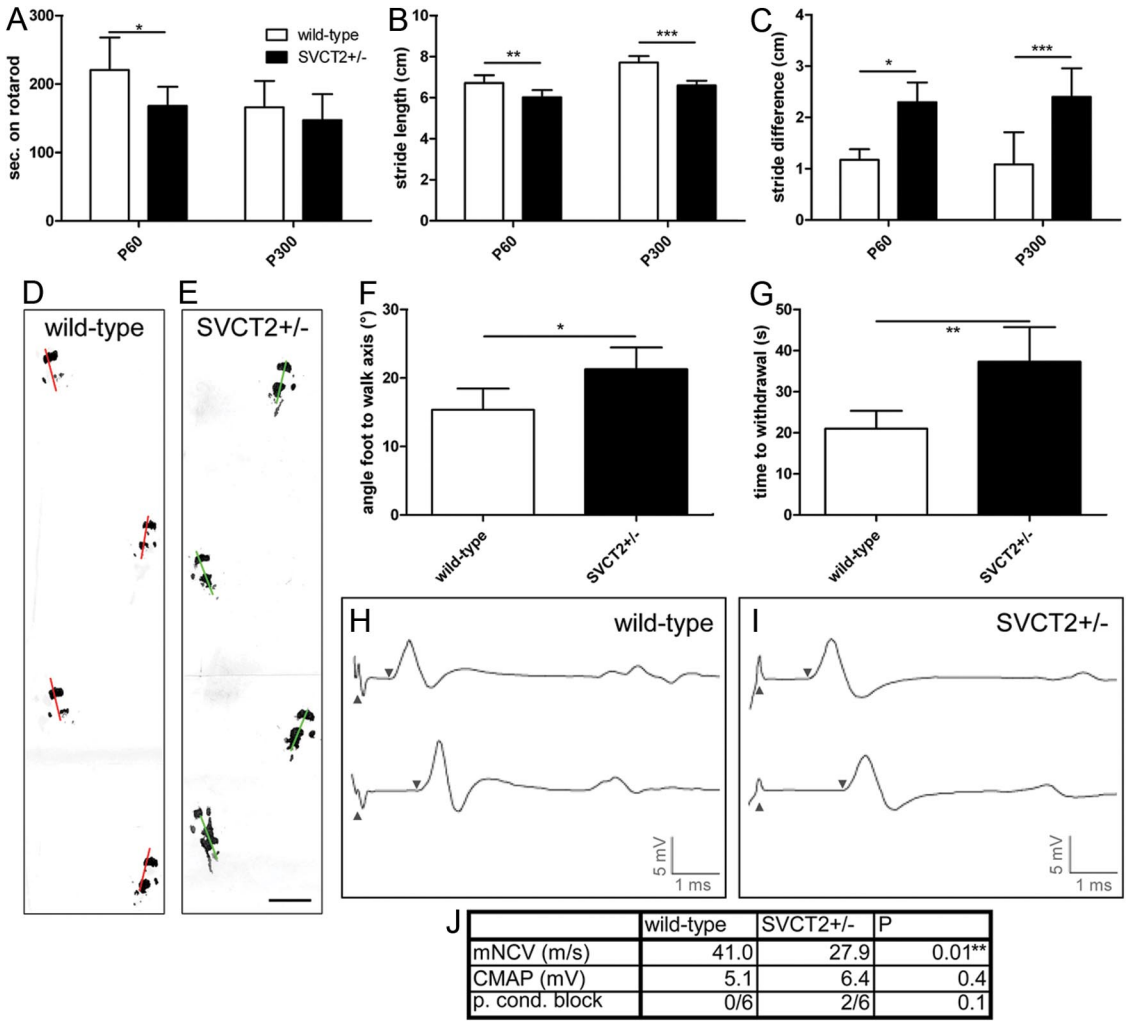

J

	wild-type	SVCT2+/-	P
mNCV (m/s)	41.0	27.9	0.01**
CMAP (mV)	5.1	6.4	0.4
p. cond. block	0/6	2/6	0.1

Figure 3. SVCT2 $^{+/-}$ mice show deficits in sensorimotor function and motor nerve conduction velocity. SVCT2 $^{+/-}$ and wild-type control mice were tested by Rotarod, gait analysis, hot plate test, and nerve conduction studies for functional assessment. ***A***, Rotarod testing showed significant reduction of performance in SVCT2 $^{+/-}$ animals at P60 (P60: $*p < 0.05$, $n = 8$). At the age of P300 both wild-type and SVCT2 $^{+/-}$ mice performed worse than at P60. There was no significant difference between the two genotypes at the age of P300 (P300: $p =$ nonsignificant, $n = 8$). ***B***, Gait analysis revealed significant reductions in stride length in SVCT2 $^{+/-}$ compared to wild-type mice at both P60 and P300 (P60: $**p < 0.01$, $n = 8$; P300: $***p < 0.001$, $n = 8$). ***C***, Gait analysis further showed a significant increase in the stride variability at both time points measured as difference between longest and shortest stride in a run (P60: $*p < 0.05$, $n = 8$; P300: $***p < 0.01$, $n = 8$). ***D***, ***E***, Representative walking tracks of a wild-type mouse (***D***) and an SVCT2 $^{+/-}$ mouse (***E***) at the age of P300 are shown with lines marking the foot-to-walk axis. ***F***, Measurements of foot-to-walk axis in P300 mice showed significantly wider stance in SVCT2 $^{+/-}$ mice compared to controls ($*p < 0.05$, $n = 8$). ***G***, In the hot plate test, SVCT2 $^{+/-}$ mice responded to the heat stimulus later than controls ($**p < 0.01$, $n = 6$), indicating a defect in nociception. ***H–J***, Nerve conduction studies were conducted to assess neurophysiological changes in SVCT2 $^{+/-}$ and wild-type peripheral nerves. ***H***, ***I***, Representative traces of sciatic nerve compound motor action potentials, CMAP, recorded from plantar foot muscles after proximal and distal stimulation (upward arrowheads) are shown. The latency until start of the CMAP is indicated by downward arrowheads. Compared to wild-type mice at P100 (***H***), age-matched SVCT2 $^{+/-}$ mice (***I***) showed temporal dispersion of CMAP amplitudes and a decrease in motor nerve conduction velocity (mNCV) ($**p < 0.01$, $n = 6$), whereas there was no change in CMAP amplitude size ($p =$ nonsignificant, $n = 6$). Partial conduction block (p. cond. block) defined as ≥50% reduction of the proximal compared to the distal CMAP amplitude was found in two of six SVCT2 $^{+/-}$ and none of six wild-type mice ($p =$ nonsignificant). Results of nerve conduction studies are summarized in table *J*.

proline hydroxylation but also by transcriptional mechanisms (Tajima and Pinnell, 1982), we were interested in collagen mRNA expression in SVCT2 $^{+/-}$ peripheral nerves. Hence, we studied the expression levels of collagen types IV, V, XV, and XXVIII mRNA in SVCT2 $^{+/-}$ and wild-type sciatic nerves. Here, we found a significant downregulation of collagen types IV, V, and XXVIII mRNA in SVCT2 $^{+/-}$ nerves at both P60 and P300. Collagen type XV showed no significant changes in SVCT2 $^{+/-}$ mice compared to wild-type mice (Fig. 5*B*).

Together, these data suggest a downregulation of MPZ in SVCT2 $^{+/-}$ nerves, while expression of the myelin protein PMP22 was not significantly affected. Furthermore, these data indicate a downregulation of various collagen types on the transcriptional level in SVCT2 $^{+/-}$ peripheral nerves.

Hydroxyproline and malondialdehyde levels are not significantly different in SVCT2 $^{+/-}$ nerves compared to wild-type controls

Ascorbic acid is a cofactor for hydroxylation of proline residues in collagen proteins (Murad et al., 1981). Hydroxyproline residues are essential for stabilization of the triple-helical conformation of collagen (Bella et al., 1994). Since ascorbic acid was reduced in SVCT2 $^{+/-}$ peripheral nerves, we investigated whether hydroxyproline levels were also decreased in SVCT2 $^{+/-}$ nerves. However, hydroxyproline assays of SVCT2 $^{+/-}$ and wild-type sciatic nerves showed no significant differences at both P60 and P300 (Fig. 6*A*). These data indicate that hydroxyproline levels are unchanged in SVCT2 $^{+/-}$ sciatic nerves, which is in agreement with previously published data on brain tissue (Sotiriou et al., 2002).

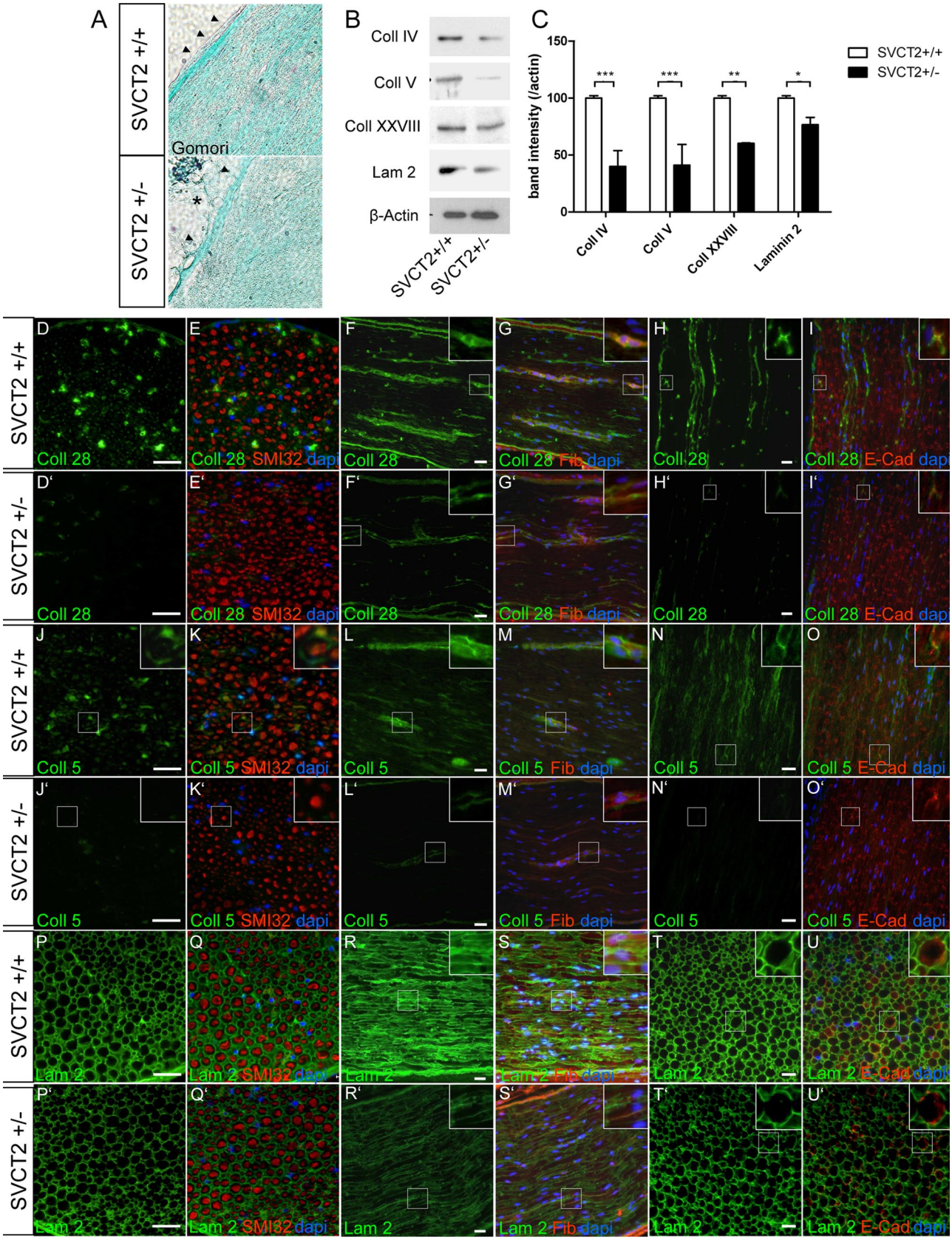

Figure 4. Formation of collagen (Coll)-containing and laminin (Lam)-containing extracellular matrix is reduced in SVCT2 $^{+/-}$ peripheral nerves. To investigate the extracellular matrix of SVCT2 $^{+/-}$ peripheral nerve tissue, we studied sciatic nerves by light microscopy, immunofluorescence microscopy, and Western blots. ***A***, Light microscopic imaging following Gomori's staining showed only mild changes in SVCT2 $^{+/-}$ nerves (bottom) compared to wild-type nerves (top). SVCT2 $^{+/-}$ nerves showed slightly disorganized collagen fibrils (green), particularly in the epineurium (arrowheads), which appeared partially disrupted (bottom image, asterisk). ***B***, Western blots of sciatic nerve lysates showed reduced band intensities for collagen IV, V, and XXVIII and for laminin-2. Actin was used as a marker for protein loading. ***C***, Densitometric analysis of Western blot bands confirmed significant downregulation of collagens IV, V, and XXVII, as well (*Figure legend continues.*)

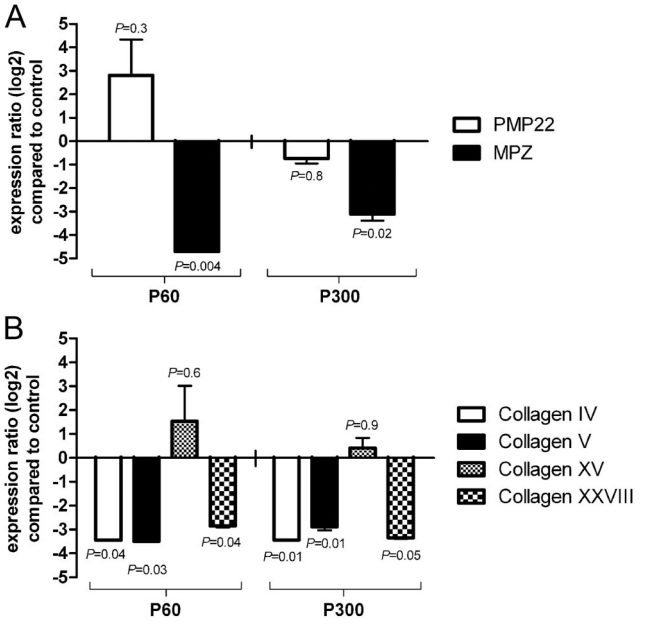

Figure 5. Expression of Myelin Protein Zero and collagen IV, V, and XXVIII mRNA is reduced in SVCT2 $^{+/-}$ sciatic nerves. To study the effect of ascorbic acid reduction on myelin and collagen gene expression, we analyzed RNA extracts of sciatic nerves by quantitative RT-PCR. Relative changes in SVCT2 $^{+/-}$ compared to wild-type nerves are shown for each gene. ***A,*** qRT-PCR of the main myelin genes MPZ and PMP22 showed significant reductions of MPZ mRNA in SVCT2 $^{+/-}$ nerves compared to wild-type nerves at both P60 and P300 (relative change: −4.7-fold and −3.1-fold, respectively). PMP22 expression showed an insignificant trend toward an upregulation at P60 (2.8-fold) and essentially no change at P300. ***B***, qRT-PCR of collagen types IV, V, XV, and XXVIII (α1 chains) showed downregulation of types IV, V, and XXVIII in SVCT2 $^{+/-}$ nerves compared to wild-types. Collagen XV mRNA concentration was not significantly changed between the two genotypes. Significance is given in the graphs; $n = 3$ for each genotype and age.

Since ascorbic acid is a known antioxidative, we sought to determine the levels of lipid peroxidation in SVCT2 $^{+/-}$ nerves. For this, we employed MDA assays, which are widely applied in the measurement of lipid peroxidation. In MDA assays, adducts are formed between MDA and thiobarbituric acid. These adducts can be quantitatively measured by spectrophotometry (Badcock et al., 1997). MDA assays of sciatic nerve lysates showed no significant differences between SVCT2 $^{+/-}$ and wild-type control nerves (Fig. 6*B*), indicating that the reduced ascorbic acid levels in SVCT2 $^{+/-}$ nerves did not lead to an increase in lipid peroxidation.

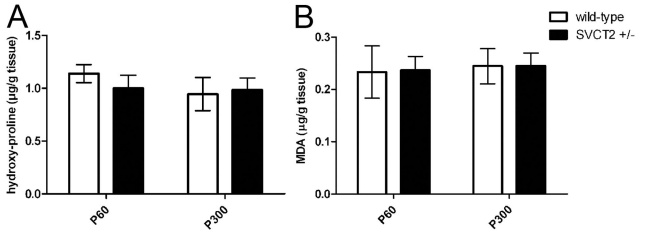

Figure 6. Malondialdehyde and hydroxyproline levels are not significantly changed in SVCT2 $^{+/-}$ compared to wild-type peripheral nerves. To assess the level of proline hydroxylation and lipid peroxidation, hydroxyproline and malondialdehyde assays were performed. ***A***, Hydroxyproline assays, performed by spectrophotometry after reaction with chloramine T and Ehrlich's reagent, showed no significant differences between SVCT2 $^{+/-}$ and wild-type sciatic nerves (P60: p = nonsignificant, $n = 3$; P300: p = nonsignificant, $n = 3$). ***B***, Malondialdehyde concentrations, as a measure for lipid peroxidation, were not significantly different between SVCT2 $^{+/-}$ and wild-type controls (P60: p = nonsignificant, $n = 3$; P300: p = nonsignificant, $n = 3$).

Collagen formation in cultured Schwann cells and myelination in Schwann cell-DRG cocultures are reduced by SVCT2-inhibition

To confirm the observation that SVCT2 deficiency leads to reduced collagen and hypomyelination in the peripheral nervous system, we used Schwann cell cultures and Schwann cell/DRG neuron cocultures in combination with SVCT2-inhibiting agents.

Primary rat Schwann cells were treated with ascorbic acid (50 μg/ml) alone or in combination with the SVCT2 inhibitor phloretin for 2 d (100 μM). Media of Schwann cell cultures were collected and processed for Western blotting. Western blots showed a significant reduction of collagen V in Schwann cell cultures treated with phloretin (Fig. 7*A*).

Since phloretin is not specific for SVCT2 but also blocks glucose transporters and other transporters, we employed siRNA to specifically inhibit SVCT2 and study the effects on collagen synthesis in Schwann cell cultures. Scrambled nonsense siRNA was used as a negative control to rule out any unspecific effects of siRNA treatment. Two days after transfection, Schwann cells were harvested for Western blotting or real-time PCR. SVCT2 siRNA-treated Schwann cell cultures showed a significant reduction in collagen V chains (Fig. 7*B*). Western blot bands of SVCT2 showed weaker bands in siRNA-treated Schwann cell cultures, confirming successful knockdown (Fig. 7*B*). Real-time PCR analysis also confirmed SVCT2 knockdown on the RNA level (Fig. 7*C*).

Next, we studied the effect of SVCT2-inhibition on myelination of DRG neurons by Schwann cells in cocultures. Schwann cell/DRG cocultures were treated with ascorbic acid alone or in combination with phloretin for 2 weeks. Myelination was assessed by immunohistochemistry with antibodies to myelin basic protein. MBP-positive segments along axons in phloretin-treated cocultures were significantly reduced in length compared to control cocultures (Fig. 7*D*, *G*, *J*). The number of MBP-positive segments was not reduced, indicating that initial Schwann cell–axon contact was not affected by SVCT2 inhibition (Fig. 7*K*). Fragmentation of axons was quantified by counting the number of axon breaks per visual field. No significant difference in the number of axon breaks was found between ascorbic acid and ascorbic acid/phloretin-treated cocultures (Fig. 7*L*). To assess the viability

←

(*Figure legend continued.*) as laminin-2 (***$p < 0.001$, **$p < 0.01$, *$p < 0.05$, $n = 3$). ***D–U′***, Immunohistochemical analysis of collagen types XXVIII, V, and laminin-2 (green) and merged images with counterstaining using neurofilament antibodies (SMI32, red), fibronectin (Fib) antibodies (red), and E-cadherin (E-Cad) antibodies (red), as well as DAPI (blue) on cryosections of sciatic nerves from SVCT2 $^{+/-}$ and wild-type mice, are shown. ***D–I′***, Immunostainings of the peripheral nerve-specific collagen type XXVIII showed reduced expression in SVCT2 $^{+/-}$ nerves (***D–I***) compared to wild-type nerves (***D′–I′***). In the wild-type nerves, collagen XXVIII was localized in the extracellular matrix as shown by double-labeling with fibronectin (***F***, ***G***, insets) and in the paranodal region of nodes of Ranvier, as shown by double-labeling with E-cadherin (***H***, ***I***, insets). In both locations, collagen XXVIII was reduced in SVCT2 $^{+/-}$ mice (***F′***, ***G′***, ***D′***, ***I′***, insets). ***J–O′***, Immunohistochemistry of collagen type V showed strong expression in wild-type nerves (***J–O***), which was markedly reduced in SVCT2 $^{+/-}$ animals (***J′–O′***). Collagen V in the extracellular matrix was strongly reduced (compare ***M*** to ***M′***, insets). Accumulation of collagen V at nodes of Ranvier was also reduced in SVCT2 $^{+/-}$ nerves (compare ***O*** to ***O′***, insets). ***P–U′***, Stainings with antibodies to laminin-2 showed a relative reduction in intensity in SVCT2 $^{+/-}$ nerves (***P′–U′***) compared to wild-types (***P–U***). Scale bars: 20 μm.

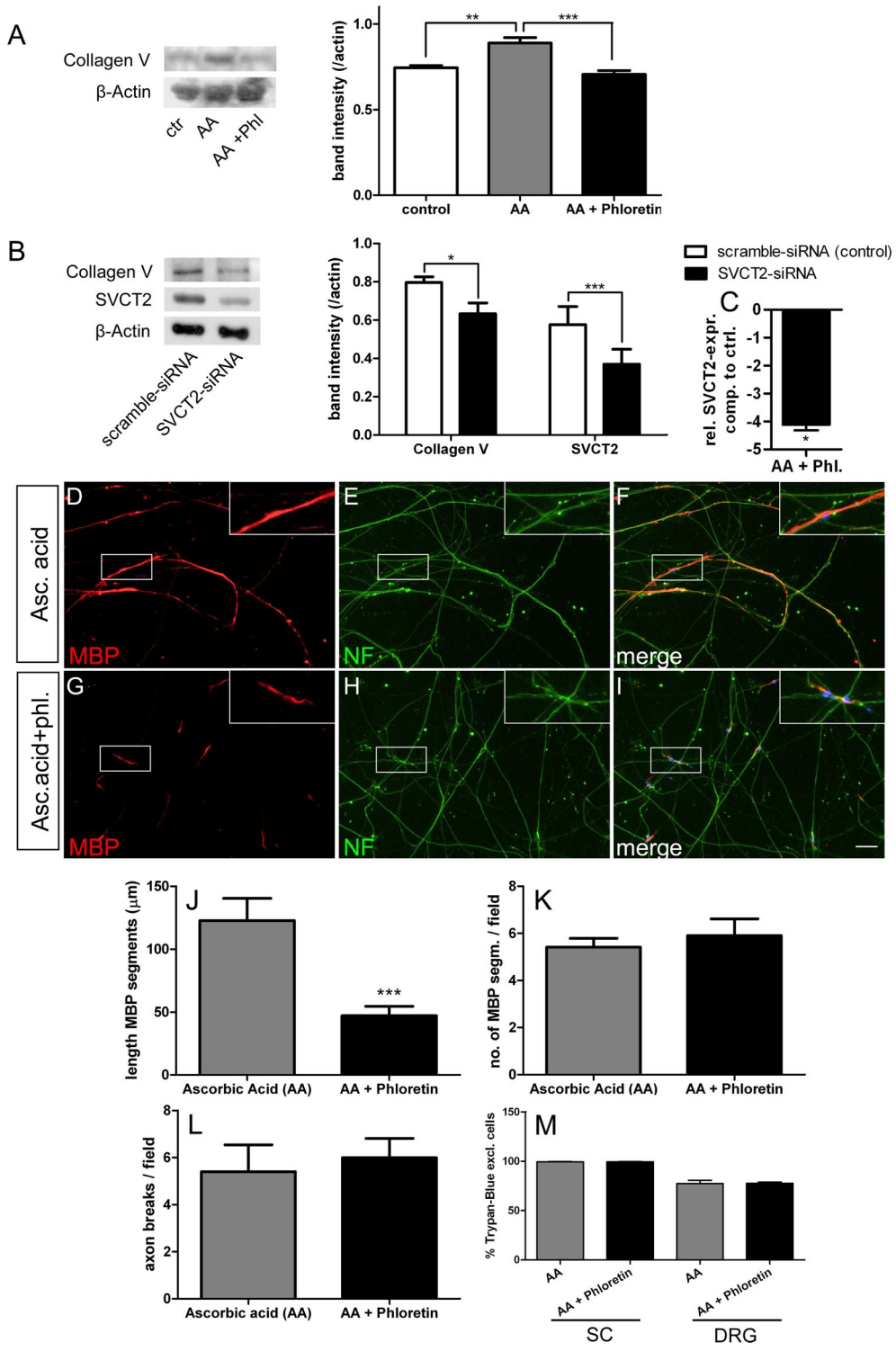

Figure 7. Extracellular collagen and myelinated segments are reduced in cell culture under SVCT2-inhibiting conditions. To test the effect of SVCT2 inhibition on collagen formation and myelination *in vitro*, we used primary Schwann cell cultures and Schwann cell/DRG cocultures. ***A***, Western blots of supernatants from Schwann cells treated with serum-free media (ctr, control), ascorbic acid (AA; 50 μg/ml), and ascorbic acid plus phloretin (AA + Phil;100 μM) showed increased collagen bands after ascorbic acid treatment that were reduced by addition of phloretin. Densitometry confirmed the increase in collagen bands by ascorbic acid treatment (**$p < 0.01$, $n = 3$), which was reduced to control levels by phloretin (***$p < 0.001$, $n = 3$). ***B***, Western blots of Schwann cell cultures treated with siRNA against SVCT2 and scrambled control siRNA showed reduced collagen bands in SVCT2-siRNA treated cultures but not in scrambled control cultures. SVCT2 bands confirmed knockdown of SVCT2 by siRNA. Densitometry confirmed these observations (collagen bands: *$p < 0.05$; SVCT2 bands: ***$p < 0.001$; $n = 3$). ***C***, Real-time PCR also confirmed the knockdown of SVCT2 on the mRNA level (*$p < 0.05$, $n = 5$) ***D–I***, Cocultures of Schwann cells and DRG neurons treated with ascorbic acid (Asc. acid; 50 μg/ml, ***D–F***) and ascorbic acid plus phloretin (Asc. acid + phl.; 100 μM, ***G–I***) were fixed and stained with MBP antibodies (***D***, ***G***, red) and neurofilament antibodies (***E***, ***H***; green). Merged images with DAPI are shown on the right (***F***, ***I***). ***J***, Myelinated segments as assessed by MBP staining were longer in ascorbic acid treated than ascorbic acid plus phloretin-treated cultures (***$p < 0.001$, $n = 5$). ***K***, The number of myelinated segments was not reduced by phloretin ($p =$ nonsignificant, $n = 5$). ***L***, The number of axon break-off points, as an indicator for damage to the neuritic network, was not different between ascorbic acid or ascorbic acid plus phloretin ($p =$ nonsignificant, $n = 5$). ***M***, The viability of both Schwann cells (SC) and DRG neurons, as assessed by Trypan blue exclusion, was not affected by phloretin ($p =$ nonsignificant, $n = 6$). Scale bar: 20 μm.

of Schwann cells and DRG neurons under treatment with phloretin, we stained cultures with Trypan blue after 2 weeks of treatment with ascorbic acid alone or in combination with phloretin. No significant differences between the two treatments were found in the proportion of viable cells in Schwann cells or DRG neurons, while viabilities were close to 100% for Schwann cells and around 77% for DRG neurons (Fig. 7*M*).

These data indicate a reduction of collagen formation and myelination by Schwann cells under SVCT2-inhibiting conditions *in vitro*, thereby confirming our observation of reduced myelin thickness and collagen expression in peripheral nerves of SVCT2$^{+/-}$ mice *in vivo*.

Discussion

In this study, we show reduced expression of SVCT2 on both transcriptional and translational level as well as decreased ascorbic acid concentrations in sciatic nerves of mice with a heterozygous knock-out of SVCT2. We provide evidence for a histopathological phenotype with reduced myelin thickness and increased G-ratios in peripheral nerves of SVCT2$^{+/-}$ mice leading to a functional phenotype with impairments in sensorimotor performance and electrophysiological tests. Furthermore, we provide evidence for defects in collagen synthesis both in SVCT2$^{+/-}$ sciatic nerves and in Schwann cell cultures under SVCT2-inhibiting conditions. Collagen mRNA levels were reduced in SVCT2$^{+/-}$ sciatic nerves, whereas the levels of hydroxyproline were unchanged, suggesting that defects in collagen synthesis occurred on the transcriptional rather than the posttranslational level.

Use of embryonic DRG/Schwann cell cocultures in this study is limited because it is difficult to translate results of embryonic DRG cultures to adult peripheral nerve pathology. In addition to the obvious difference in the developmental stages of the two systems, there is also a tremendous difference in cell biological complexity (e.g., lack of fibroblasts and immune cells in DRG/Schwann cell cocultures).

Recently, several studies revealed the expression and transport activity of SVCT2 in a variety of nervous system compartments and cell types (Castro et al., 2001; Angelow et al., 2003; Garcia Mde et al., 2005; Mun et al., 2006; Qiu et al., 2007; Caprile et al., 2009; Harrison and May, 2009; Gess et al., 2011). We previously showed expression and activity of SVCT2 in Schwann cell cultures *in vitro* (Gess et al., 2010). However, the functional relevance of SVCT2 for the peripheral nervous system was not shown so far. Furthermore, there was no *in vivo* evidence for a function of ascorbic acid in peripheral nerve myelination.

In this study, we show for the first time that SVCT2 is necessary for ascorbic acid uptake into the peripheral nervous system *in vivo*. Our results show that reduction of SVCT2 expression in SVCT2$^{+/-}$ mice leads to a 30–50% decrease in the concentration of ascorbic acid in the sciatic nerve. This suggests that SVCT2 is functionally relevant for the transport of ascorbic acid into peripheral nerves *in vivo*. It cannot be excluded that the reduction in peripheral nerve ascorbic acid is due to the reduced ascorbic acid levels in the blood of SVCT2$^{+/-}$ mice and not due to a relative SVCT2-deficiency in peripheral nerves themselves. However, in the study by Sotiriou et al. (2002) significant differences in the overall amount of ascorbic acid were not found in organs and tissues throughout the organism of SVCT2$^{+/-}$ mice, but only in specific locations like the brain. The brain is known to contain much higher levels of ascorbic acid than the systemic circulation and most organs (Schenk et al., 1982; Harrison et al., 2010b). This indicates that SVCT2 heterozygosity does not lead to a general reduction of ascorbic acid concentration in all tissues but only in those that establish high ascorbic acid concentrations and are more sensitive to SVCT2 gene dosage. Our study provides the first available data on ascorbic acid concentrations in peripheral nerves *in vivo*, showing that ascorbic acid concentrations in peripheral nerves are high compared to those in other tissues. In wild-type sciatic nerves we found ascorbic acid concentrations of 2.3–3.1 μmol/g. These values are in the range of previously reported values for adult mouse brain (2.0–4.2 μmol/g) and just below those for fetal mouse brain (2.9–4.0 μmol/g) and fetal rat brain (3.6–4.0 μmol/g) (Kratzing et al., 1985; Kuo et al., 2004; Harrison et al., 2010a, 2010c. Since peripheral nerves contain as much ascorbic acid as brain tissue, it appears that the peripheral nerve is equally ascorbic acid-privileged as the brain, which supports the assumption that ascorbic acid may have important functions in the peripheral nervous system. Indeed, SVCT2$^{+/-}$ sciatic nerves fibers exhibited reduced myelin thickness and thereby increased G-ratios, suggesting a function of ascorbic acid in peripheral nerve myelination *in vivo*. The demyelinating histological phenotype was shown to cause deficits in motor function, sensory function, and nerve conduction velocity. The delay in the response to thermal stimulation in SVCT2$^{+/-}$ mice may indicate that thinly myelinated Aδ-fibers, which are known to mediate acute pain sensation leading to limb withdrawal, were affected by the demyelinating phenotype. On the other hand, as Remak bundle architecture was changed in SVCT2$^{+/-}$ mice, an impairment of the function of nonmyelinated C fibers may also provide an explanation for the change in withdrawal to thermal stimulation.

As we show deficiencies of various collagen types, especially of collagen V, in SVCT2$^{+/-}$ peripheral nerves and SVCT2-inhibited Schwann cell cultures, the specific function of ascorbic acid in the peripheral nerve might be the regulation of collagen formation. Several collagen types have been shown to be expressed in peripheral nerves: collagen I, III, IV, V, XV, and XXVIII (Osawa and Ide, 1986; Chernousov et al., 2006; Grimal et al., 2010; Rasi et al., 2010). Collagen IV and XV are basement membrane collagens, while collagen I, III, and V are fibril-forming collagens. Collagen XXVIII is an atypical collagen specifically expressed in the peripheral nervous system (Veit et al., 2006; Plumb et al., 2007; Grimal et al., 2010). A functional relevance in the peripheral nerve has been shown for collagen V, which is necessary for myelination in SC/DRG cocultures *in vitro* (Chernousov et al., 2006), and collagen XV, the lack of which has been shown to cause peripheral nerve defects when combined with laminin deficiency (Rasi et al., 2010). Of the collagens expressed in the peripheral nervous system, we studied collagen IV (a basement membrane collagen), collagen V (a fibril forming collagen), and the specific collagen XXVIII. Reductions of collagen IV, V, and XXVIII to about 50% of control were detected in SVCT2$^{+/-}$ nerves by immunohistochemistry and Western blots. By qRT-PCR, collagen IV, V, and XXVIII expression was shown to be reduced 3-fold to 4-fold in SVCT2$^{+/-}$ sciatic nerves. Thus, the rates of downregulation of collagen types were considerably higher in qRT-PCR than in Western blots. This discrepancy may be due to posttranslational mechanisms that stabilize collagen proteins, so that a reduction of mRNA transcripts does not lead to an equal reduction of protein. On the other hand, the discrepancy between qRT-PCR and Western blots may be due to the different sensitivity and specificity of the two methods, making qRT-PCR more sensitive to relative expression changes than Western blots.

To the contrary, hydroxyproline levels were unchanged in SVCT2$^{+/-}$ nerves compared to wild-type nerves. This is in ac-

cordance with previous studies on SVCT2 $^{-/-}$ fetuses, in which no decrease of hydroxyproline levels was found despite severe vitamin C deficiency (Sotiriou et al., 2002). These results suggest that ascorbic acid is necessary for collagen synthesis in peripheral nerves and that collagen, in turn, is necessary for correct myelination. Furthermore, our data suggest that ascorbic acid regulates collagen formation by transcriptional mechanisms rather than through proline hydroxylation. Possibly, collagen transcription is more sensitive to relative changes in ascorbic acid concentration than proline hydroxylation so that a 30–50% decrease in ascorbic acid concentration—as observed in our studies—affects collagen transcription but not proline hydroxylation. Interestingly, transcriptional regulation of collagen by ascorbic acid was previously shown in skin fibroblasts. This regulation was independent of the effect of ascorbic acid on proline hydroxylation (Tajima and Pinnell, 1982, 1996; Geesin et al., 1988).

Our results showed a trend toward increased PMP22 mRNA levels in SVCT2 $^{+/-}$ peripheral nerves at P60 (although not significant) and unchanged levels at P300. This is interesting with respect to previously published data on ascorbic acid treatment of a PMP22 transgenic mouse line in which overexpressed PMP22 was downregulated by ascorbic acid (Passage et al., 2004). The slight but insignificant increase in PMP22 expression at P60 we observed would fit to these data. The unchanged PMP22 expression level at P300 would not be in accordance with the study by Passage et al. (2004). However, caution should be advised in comparing these two studies, since very different animal models were used.

MPZ expression was shown to be reduced in our studies at P60 and P300 in SVCT2 $^{+/-}$ compared to wild-type sciatic nerves. As MPZ is the most abundant peripheral myelin protein, this downregulation is most likely a consequence of the hypomyelination of the peripheral nerve. Thus, MPZ downregulation might be a secondary effect caused by reduced extracellular collagen. Interactions between extracellular matrix components and myelin gene expression have been proposed, although the molecular mechanisms have not been revealed so far (Chen and Strickland, 2003; Chernousov et al., 2006, 2008). Alternatively, MPZ downregulation may be a direct effect of reduced ascorbic acid. However, to our knowledge an effect of ascorbic acid on MPZ mRNA or protein expression has not been described in the literature.

In conclusion, we find reduced ascorbic acid concentrations, hypomyelination, and defects in collagen formation in peripheral nerves of SVCT2 $^{+/-}$ mice leading to sensorimotor impairments. Reduced collagen expression and myelination were further shown in Schwann cell cultures and Schwann cell/DRG cocultures under SVCT2-inhibiting conditions. These results will help to elucidate the mechanism of ascorbic acid transport into peripheral nerves and the function of ascorbic acid in myelination and myelin maintenance in the peripheral nervous system. A better understanding of the transport mechanisms of ascorbic acid and pharmacological manipulation of SVCT2 may lead to the development of novel therapeutic approaches to peripheral neuropathies.

References

Angelow S, Haselbach M, Galla HJ (2003) Functional characterisation of the active ascorbic acid transport into cerebrospinal fluid using primary cultured choroid plexus cells. Brain Res 988:105–113.

Badcock NR, Zoanetti GD, Martin ES (1997) Nonchromatographic assay for malondialdehyde-thiobarbituric acid adduct with HPLC equivalence. Clin Chem 43:1655–1657.

Bella J, Eaton M, Brodsky B, Berman HM (1994) Crystal and molecular structure of a collagen-like peptide at 1.9 Å resolution. Science 266:75–81.

Booth BA, Uitto J (1981) Collagen biosynthesis by human skin fibroblasts. III. The effects of ascorbic acid on procollagen production and prolyl hydroxylase activity. Biochim Biophys Acta 675:117–122.

Burns J, Ouvrier RA, Yiu EM, Joseph PD, Kornberg AJ, Fahey MC, Ryan MM (2009) Ascorbic acid for Charcot-Marie-Tooth disease type 1A in children: a randomised, double-blind, placebo-controlled, safety and efficacy trial. Lancet Neurol 8:537–544.

Caprile T, Salazar K, Astuya A, Cisternas P, Silva-Alvarez C, Montecinos H, Millán C, de Los Angeles García M, Nualart F (2009) The Na+-dependent L-ascorbic acid transporter SVCT2 expressed in brainstem cells, neurons, and neuroblastoma cells is inhibited by flavonoids. J Neurochem 108:563–577.

Carey DJ, Todd MS (1987) Schwann cell myelination in a chemically defined medium: demonstration of a requirement for additives that promote Schwann cell extracellular matrix formation. Brain Res 429:95–102.

Castro M, Caprile T, Astuya A, Millán C, Reinicke K, Vera JC, Vásquez O, Aguayo LG, Nualart F (2001) High-affinity sodium-vitamin C co-transporters (SVCT) expression in embryonic mouse neurons. J Neurochem 78:815–823.

Chen ZL, Strickland S (2003) Laminin gamma1 is critical for Schwann cell differentiation, axon myelination, and regeneration in the peripheral nerve. J Cell Biol 163:889–899.

Chernousov MA, Rothblum K, Stahl RC, Evans A, Prentiss L, Carey DJ (2006) Glypican-1 and alpha4(V) collagen are required for Schwann cell myelination. J Neurosci 26:508–517.

Chernousov MA, Yu WM, Chen ZL, Carey DJ, Strickland S (2008) Regulation of Schwann cell function by the extracellular matrix. Glia 56:1498–1507.

Cosgaya JM, Chan JR, Shooter EM (2002) The neurotrophin receptor p75NTR as a positive modulator of myelination. Science 298:1245–1248.

Eldridge CF, Bunge MB, Bunge RP, Wood PM (1987) Differentiation of axon-related Schwann cells in vitro. I. Ascorbic acid regulates basal lamina assembly and myelin formation. J Cell Biol 105:1023–1034.

Eldridge CF, Bunge MB, Bunge RP (1989) Differentiation of axon-related Schwann cells in vitro: II. Control of myelin formation by basal lamina. J Neurosci 9:625–638.

Fleming SM, Chesselet M (2005) Phenotypical characterization of genetic mouse models of Parkinson disease. In: Animal models of movement disorders (LeDoux M, ed), pp 183–192. London: Elsevier.

García Mde L, Salazar K, Millán C, Rodríguez F, Montecinos H, Caprile T, Silva C, Cortes C, Reinicke K, Vera JC, Aguayo LG, Olate J, Molina B, Nualart F (2005) Sodium vitamin C cotransporter SVCT2 is expressed in hypothalamic glial cells. Glia 50:32–47.

Garratt AN, Voiculescu O, Topilko P, Charnay P, Birchmeier C (2000) A dual role of erbB2 in myelination and in expansion of the Schwann cell precursor pool. J Cell Biol 148:1035–1046.

Geesin JC, Darr D, Kaufman R, Murad S, Pinnell SR (1988) Ascorbic acid specifically increases type I and type III procollagen messenger RNA levels in human skin fibroblast. J Invest Dermatol 90:420–424.

Gess B, Halfter H, Kleffner I, Monje P, Athauda G, Wood PM, Young P, Wanner IB (2008) Inhibition of N-cadherin and beta-catenin function reduces axon-induced Schwann cell proliferation. J Neurosci Res 86:797–812.

Gess B, Lohmann C, Halfter H, Young P (2010) Sodium-dependent vitamin C transporter 2 (SVCT2) is necessary for the uptake of L-ascorbic acid into Schwann cells. Glia 58:287–299.

Gess B, Sevimli S, Strecker JK, Young P, Schäbitz WR (2011) Sodium-dependent vitamin C transporter 2 (SVCT2) expression and activity in brain capillary endothelial cells after transient ischemia in mice. PLoS One 6:e17139.

Grimal S, Puech S, Wagener R, Ventéo S, Carroll P, Fichard-Carroll A (2010) Collagen XXVIII is a distinctive component of the peripheral nervous system nodes of ranvier and surrounds nonmyelinating glial cells. Glia 58:1977–1987.

Harrison FE, May JM (2009) Vitamin C function in the brain: vital role of the ascorbate transporter SVCT2. Free Radic Biol Med 46:719–730.

Harrison FE, May JM, McDonald MP (2010a) Vitamin C deficiency increases basal exploratory activity but decreases scopolamine-induced activity in APP/PSEN1 transgenic mice. Pharmacol Biochem Behav 94:543–552.

Harrison FE, Green RJ, Dawes SM, May JM (2010b) Vitamin C distribution and retention in the mouse brain. Brain Res 1348:181–186.

Harrison FE, Dawes SM, Meredith ME, Babaev VR, Li L, May JM (2010c) Low vitamin C and increased oxidative stress and cell death in mice that lack the sodium-dependent vitamin C transporter SVCT2. Free Radic Biol Med 49:821–829.

Karatas F, Karatepe M, Baysar A (2002) Determination of free malondialdehyde in human serum by high-performance liquid chromatography. Anal Biochem 311:76–79.

Kratzing CC, Kelly JD, Kratzing JE (1985) Ascorbic acid in fetal rat brain. J Neurochem 44:1623–1624.

Kuo SM, MacLean ME, McCormick K, Wilson JX (2004) Gender and sodium-ascorbate transporter isoforms determine ascorbate concentrations in mice. J Nutr 134:2216–2221.

Low PA, McLeod JG, Prineas JW (1978) Hypertrophic Charcot-Marie-Tooth disease. Light and electron microscope studies of the sural nerve. J Neurol Sci 35:93–115.

Micallef J, Attarian S, Dubourg O, Gonnaud PM, Hogrel JY, Stojkovic T, Bernard R, Jouve E, Pitel S, Vacherot F, Remec JF, Jomir L, Azabou E, Al-Moussawi M, Lefebvre MN, Attolini L, Yaici S, Tanesse D, Fontes M, Pouget J, Blin O (2009) Effect of ascorbic acid in patients with Charcot-Marie-Tooth disease type 1A: a multicentre, randomised, double-blind, placebo-controlled trial. Lancet Neurol 8:1103–1110.

Mun GH, Kim MJ, Lee JH, Kim HJ, Chung YH, Chung YB, Kang JS, Hwang YI, Oh SH, Kim JG, Hwang DH, Shin DH, Lee WJ (2006) Immunohistochemical study of the distribution of sodium-dependent vitamin C transporters in adult rat brain. J Neurosci Res 83:919–928.

Murad S, Grove D, Lindberg KA, Reynolds G, Sivarajah A, Pinnell SR (1981) Regulation of collagen synthesis by ascorbic acid. Proc Natl Acad Sci U S A 78:2879–2882.

Olsen CL, Bunge RP (1986) Requisites for growth and myelination of urodele sensory neurons in tissue culture. J Exp Zool 238:373–384.

Osawa T, Ide C (1986) Changes in thickness of collagen fibrils in the endo- and epineurium of the mouse sciatic nerve during development. Acta Anat 125:245–251.

Pareyson D, Reilly MM, Schenone A, Fabrizi GM, Cavallaro T, Santoro L, Vita G, Quattrone A, Padua L, Gemignani F, Visioli F, Laurà M, Radice D, Calabrese D, Hughes RA, Solari A (2011) Ascorbic acid in Charcot-Marie-Tooth disease type 1A (CMT-TRIAAL and CMT-TRAUK): a double-blind randomised trial. Lancet Neurol 10:320–328.

Passage E, Norreel JC, Noack-Fraissignes P, Sanguedolce V, Pizant J, Thirion X, Robaglia-Schlupp A, Pellissier JF, Fontés M (2004) Ascorbic acid treatment corrects the phenotype of a mouse model of Charcot-Marie-Tooth disease. Nat Med 10:396–401.

Pfaffl MW (2001) A new mathematical model for relative quantification in real-time RT-PCR. Nucleic Acids Res 29:e45.

Pfaffl MW, Horgan GW, Dempfle L (2002) Relative expression software tool (REST) for group-wise comparison and statistical analysis of relative expression results in real-time PCR. Nucleic Acids Res 30:e36.

Plumb DA, Dhir V, Mironov A, Ferrara L, Poulsom R, Kadler KE, Thornton DJ, Briggs MD, Boot-Handford RP (2007) Collagen XXVII is developmentally regulated and forms thin fibrillar structures distinct from those of classical vertebrate fibrillar collagens. J Biol Chem 282:12791–12795.

Qiu S, Li L, Weeber EJ, May JM (2007) Ascorbate transport by primary cultured neurons and its role in neuronal function and protection against excitotoxicity. J Neurosci Res 85:1046–1056.

Rasi K, Hurskainen M, Kallio M, Stavén S, Sormunen R, Heape AM, Avila RL, Kirschner D, Muona A, Tolonen U, Tanila H, Huhtala P, Soininen R, Pihlajaniemi T (2010) Lack of collagen XV impairs peripheral nerve maturation and, when combined with laminin-411 deficiency, leads to basement membrane abnormalities and sensorimotor dysfunction. J Neurosci 30:14490–14501.

Schenk JO, Miller E, Gaddis R, Adams RN (1982) Homeostatic control of ascorbate concentration in CNS extracellular fluid. Brain Res 253:353–356.

Sereda M, Griffiths I, Pühlhofer A, Stewart H, Rossner MJ, Zimmerman F, Magyar JP, Schneider A, Hund E, Meinck HM, Suter U, Nave KA (1996) A transgenic rat model of Charcot-Marie-Tooth disease. Neuron 16:1049–1060.

Sotiriou S, Gispert S, Cheng J, Wang Y, Chen A, Hoogstraten-Miller S, Miller GF, Kwon O, Levine M, Guttentag SH, Nussbaum RL (2002) Ascorbic-acid transporter Slc23a1 is essential for vitamin C transport into the brain and for perinatal survival. Nat Med 8:514–517.

Tajima S, Pinnell SR (1982) Regulation of collagen synthesis by ascorbic acid. Ascorbic acid increases type I procollagen mRNA. Biochem Biophys Res Commun 106:632–637.

Tajima S, Pinnell SR (1996) Ascorbic acid preferentially enhances type I and III collagen gene transcription in human skin fibroblasts. J Dermatol Sci 11:250–253.

Veit G, Kobbe B, Keene DR, Paulsson M, Koch M, Wagener R (2006) Collagen XXVIII, a novel von Willebrand factor A domain-containing protein with many imperfections in the collagenous domain. J Biol Chem 281:3494–3504.

Verhamme C, de Haan RJ, Vermeulen M, Baas F, de Visser M, van Schaik IN (2009) Oral high dose ascorbic acid treatment for one year in young CMT1A patients: a randomised, double-blind, placebo-controlled phase II trial. BMC Med 7:70.

Vroemen M, Weidner N (2003) Purification of Schwann cells by selection of p75 low affinity nerve growth factor receptor expressing cells from adult peripheral nerve. J Neurosci Methods 124:135–143.

Woessner JF Jr (1961) The determination of hydroxyproline in tissue and protein samples containing small proportions of this imino acid. Arch Biochem Biophys 93:440–447.

Young P, Boussadia O, Berger P, Leone DP, Charnay P, Kemler R, Suter U (2002) E-cadherin is required for the correct formation of autotypic adherens junctions of the outer mesaxon but not for the integrity of myelinated fibers of peripheral nerves. Mol Cell Neurosci 21:341–351.